LSO/LYSO Crystals for Calorimeters in Future HEP Experiments

Liyuan Zhang, *Member, IEEE*, Rihua Mao, *Member, IEEE*, Fang Yang, *Member, IEEE*, and Ren-Yuan Zhu, *Senior Member, IEEE*

***Abstract*—Because of their high stopping power ($X_0 = 1.14$ cm), fast ($\tau = 40$ ns) bright (4 times BGO) scintillation with small temperature coefficient ($-0.2\%/^\circ C$) and superb radiation hardness, LSO/LYSO crystals are chosen to construct electromagnetic calorimeters (ECAL) of total absorption nature. One critical issue for this application is the light response uniformity (LRU) of long crystal bars with tapered geometry, which is affected by the non-uniform light yield along the crystal, the self-absorption and the optical focusing effect. Following a ray-tracing simulation study, an uniformization method was developed by roughening one side surface with LRU of better than 3% achieved. LSO/LYSO crystals are also proposed as the active material for a sampling ECAL for future HEP experiments in severe radiation environment. Preliminary designs with Pb or W absorber are described. Measurements of light collection efficiency (LCE) for prototype Shashlik cells with wavelength shifting fiber readout are presented. Future development on LSO/LYSO crystal based sampling ECAL is discussed.**

***Index Terms*—Crystal, emission, light attenuation length, light output, light response uniformity (LRU), ray-tracing, sampling calorimeter, scintillator, Shashlik, transmittance.**

I. Introduction

BECAUSE of their high stopping power ($X_0 = 1.14$ cm), fast ($\tau = 40$ ns) and bright (4 times BGO) scintillation [1]–[3] [17] with a low temperature coefficient ($-0.2\%/$ °C) [4] and superb radiation hardness against gamma-rays [5], neutrons [6] and charged hadrons [7] cerium doped lutetium oxyorthosilicate (Lu_2SiO_5 : Ce, LSO) and lutetium yttrium oxyorthosilicate ($Lu_{2(1-x)}Y_{2x}SiO_5$: Ce, LYSO) crystals have attracted a broad interest in the high energy physics community. As a result, LSO/LYSO crystals have been chosen by the Mu2e and SuperB experiments to construct total absorption electromagnetic calorimeters (ECAL). LSO/LYSO crystal based sampling ECAL has also been proposed for future HEP experiments in severe radiation environment, such as the CMS endcap ECAL upgrade for the HL-LHC.

A crucial issue for an LSO/LYSO based total absorption ECAL is the light response uniformity (LRU) of long crystal bars with tapered geometry, which is affected by three factors: (1) the non-uniform light yield along the crystal length, caused by the non-uniform cerium concentration because of the cerium segregation; (2) the self-absorption caused by the interplay between emission and transmission, and (3) the optical focusing effect caused by the tapered geometry. For LSO/LYSO crystal based sampling calorimeter detector concepts a crucial issue is the light collection efficiency (LCE).

This paper presents results of a R&D program carried out in the Caltech Crystal Lab for LSO/LYSO crystal based ECALs for future HEP experiments. Section II describes a uniformization method by roughening one side surface of LSO/LYSO crystals with tapered geometry. The result LRU of better than 3% was achieved for twenty five 20 cm long LYSO crystals with APD readout. Section III describes two LSO/LYSO crystal based sampling ECAL detector concepts, their preliminary design parameters with Pb or W absorber, and the LCE measurements for the Shashlik concept with wavelength shifting (WLS) fiber readout. Future development on LSO/LYSO crystal based sampling ECAL is discussed.

Manuscript received May 24, 2013; revised August 09, 2013; accepted August 26, 2013. Date of publication October 17, 2013; date of current version February 06, 2014. This work was supported in part by the U.S. Department of Energy under Grant DE-FG03-92-ER-40701.

The authors are with the California Institute of Technology, Pasadena, CA 91125 USA (e-mail: zhu@hep.caltech.edu).

Color versions of one or more of the figures in this paper are available online at http://ieeexplore.ieee.org.

Digital Object Identifier 10.1109/TNS.2013.2279993

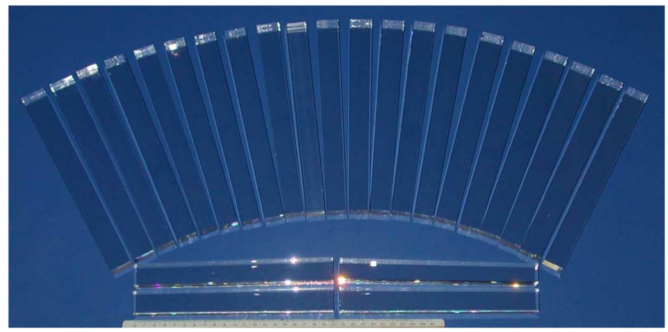

Fig. 1. Twenty five LYSO crystals with tapered geometry.

II. Optimization of Light Response Uniformity

Fig. 1 shows twenty five LYSO crystals of 20 cm long with tapered geometry of about 20×20 mm^2 at the small end and 23×23 mm^2 at the large end for a test beam matrix of the SuperB experiment. They were grown by Czochralski method at Saint-Gobain (SG) Corporation, Shanghai Institute of Ceramics (SIC) and Sichuan Institute of Piezoelectric and Acousto-optic Technology (SIPAT). All instruments and set-ups used for the measurements presented in this section are described in our previous publications, e.g. [8].

The initial LRU was measured by a pair of Hamamatsu S8664-55 APDs with collimated γ-rays shooting longitudinally along the crystal [8]. The corresponding non-uniformity is parameterized as the δ value by a linear fit, as shown in Fig. 2, where Y_{mid} is the fitted value of the light output at the middle of the crystal (X_{mid}). While the LRUs measured for crystals

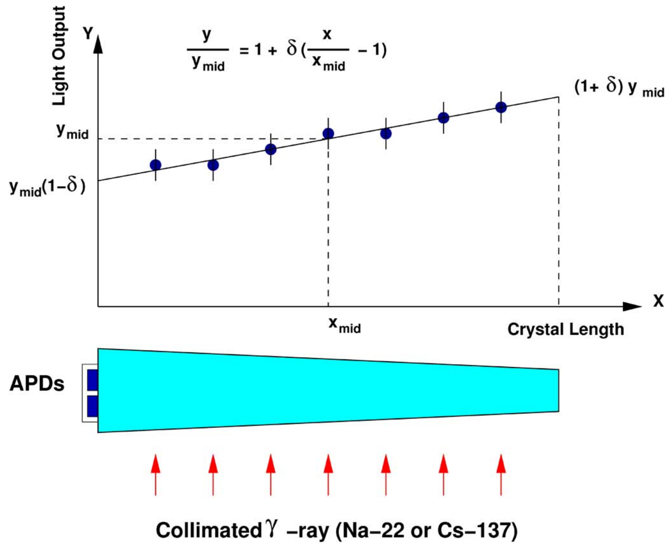

Fig. 2. Schematic showing the light response uniformity measurement.

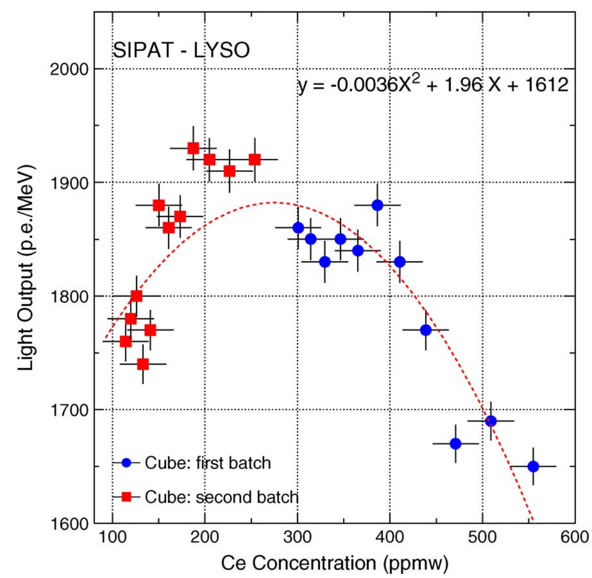

Fig. 3. LYSO light output as function of the Ce concentration in PPMW.

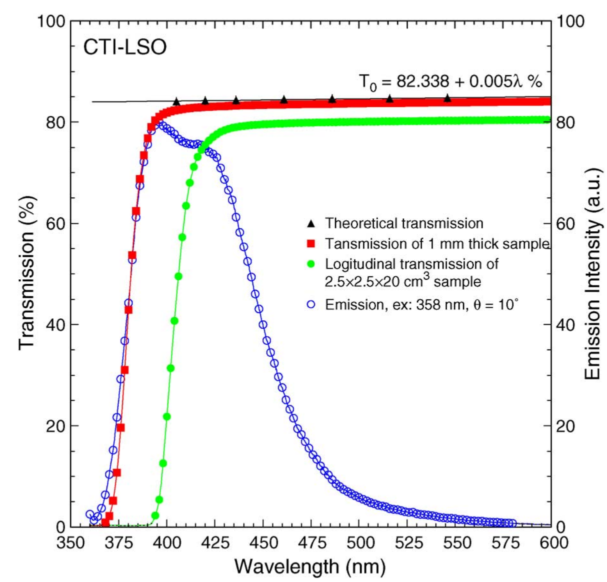

Fig. 4. Emission and transmittance spectra of a 20 cm long and an 1 mm thick LSO crystals are shown as a function of wavelength. Also shown are the theoretical limits of the transmittance (black triangles) assuming multiple reflections inside the crystal and no internal absorption.

from different vendors are slightly different, their average value is about 10%, which exceeds the 3% required for SuperB crystals of 18 X_0 length to maintain the excellent intrinsic energy resolution offered by the LSO/LYSO crystals.

There three factors which affect the measured LRU values. First, there is a variation of the cerium concentration along the crystal length. Because of the segregation during crystal growth, the cerium concentration is not uniform along the crystal length. Fig. 3 shows the light yield as a function of the Ce concentration for two batches of LYSO cubes cut from two ingots grown with different level of initial cerium doping. All cubes are of the same dimension 17 mm with six faces polished and wrapped with Tyvek paper when their light output was measured by using a ^{137}Cs source and a PMT R1306 [8]. After the light output measurements, the cerium concentration in these samples was determined by using Glow Discharge Mass Spectroscopy (GDMS) analysis in Northern Analytical Laboratory, Inc. [9]. The result of these measurements shows an increase of the light output when the cerium concentration is small and a decrease when the cerium concentration is too large. An optimized cerium concentration range in LSO/LYSO crystals is found to be between 150 to 400 PPMW.

The LRU is also affected by the self-absorption effect of the scintillation light in LSO/LYSO crystals. Fig. 4 shows the longitudinal transmittance spectra measured for two LSO samples of 20 cm and 1 mm long together with the theoretical limits of the transmittance (black triangles) assuming multiple reflections inside the crystal and no internal absorption [10]. Also shown in the figure is the photo-luminescence spectrum without internal absorption [11]. It is clear that a part of the scintillation emission is absorbed inside the crystal, causing a large difference in the transmittance spectra measured for two crystals with different light path length. This self-absorption effect was discussed in details in our previous publications, e.g. [12].

Fig. 5 shows the light attenuation length (LAL) as a function of wavelength, which is calculated by using the theoretical limits of the transmittance and the measured longitudinal transmittance of the 20 cm long sample [4], [10], as well as the emission spectrum. Also shown in the figure is the emission weighted light attenuation length (EWLAL). It is clear that the LAL is very much wavelength dependent between 380 and 500 nm within the emission spectrum. This wavelength dependent light attenuation length must be used for an appropriate ray-tracing simulation in LSO/LYSO crystals.

The last, but not the least, factor affects the LRU is the crystal shape. It is well known that the light collection efficiency (LCE) is longitudinal position dependent in a tapered crystal. With the large end of a tapered crystal coupled to a photo-detector, the LCE at the small (or far) end is higher than the large (or near) end because of the total reflection inside the crystal, which is usually called the optical focusing effect. A ray-tracing simulation was

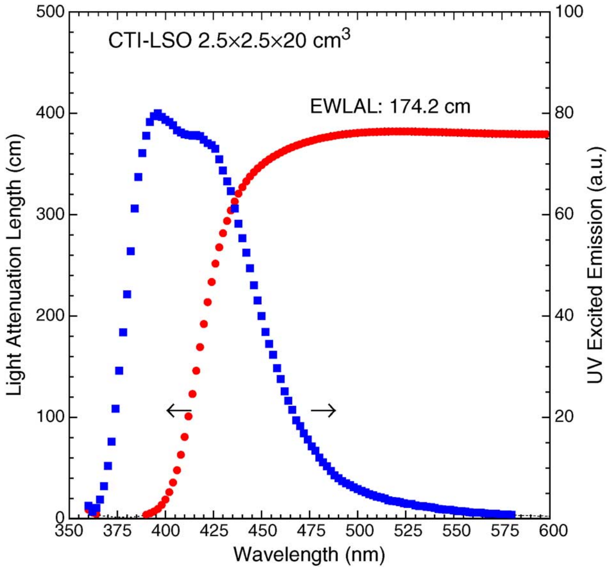

Fig. 5. Emission spectrum and the light attenuation length are shown as a function of wavelength.v

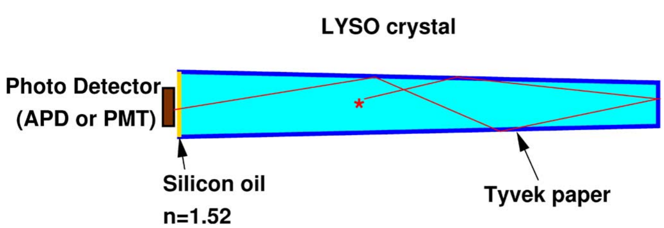

Fig. 6. Set-up used for the ray-tracing simulation described in the text.

carried out to understand all these three effects with the set-up shown in Fig. 6.

Photons were generated isotropically in a cross-section at a defined distance (z) to the photo-detector, and were propagated inside the entire crystal volume until either reaching the photo-detector or escaping from the crystal volume. The weight of each photon reaching the photo-detector was calculated according to the integrated light path length and the LAL, which is a function of wavelength (λ). The light collection efficiency (LCE) as a function of λ and z, $\mathrm{LCE}(\lambda, \mathrm{z})$, was calculated by summing all weights of photons reaching the photo-detector and normalized to the total number of photons generated. This was repeated for seven z positions along the crystal and for different wavelength. Finally, the light output (LO) as a function z, LO(z), was calculated by imposing the non-uniform light yield along the crystal, LY(z), on the integration of the emission spectrum, $\mathrm{Em}(\lambda)$, the light collection efficiency, $\mathrm{LCE}(\lambda, \mathrm{z})$ and the quantum efficiency of the photo-detector, $\mathrm{QE}(\lambda)$, according to

$$LO(z) = LY(z) \int Em(\lambda) LCE(\lambda, z) QE(\lambda) d\lambda. \quad (1)$$

The simulation result shows that the cerium concentration and self-absorption may compensate each other by coupling an appropriate end of a long rectangular crystal to the photo-detector. The 10% non-uniformity observed in SuperB crystals is actually dominated by the optical focusing effect. Fig. 7 shows the light output of a SuperB crystal as a function of the distance

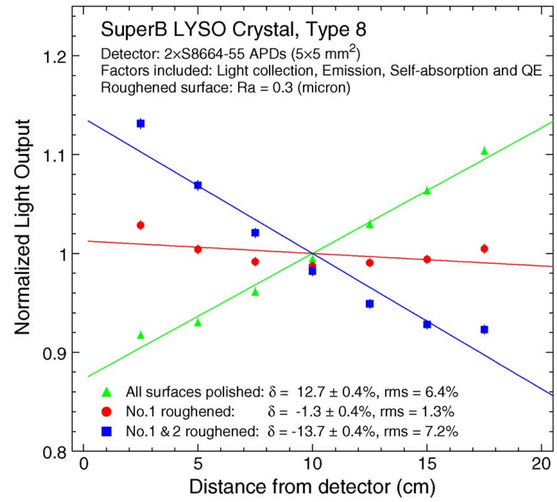

Fig. 7. Light output of a SuperB type 8 crystal is shown as a function of the distance to the photo-detector with (1) all surfaces polished; (2) one surface roughened to $\mathrm{R}_a = 0.3$ and (3) two surfaces roughened to $\mathrm{R}_a = 0.3$.

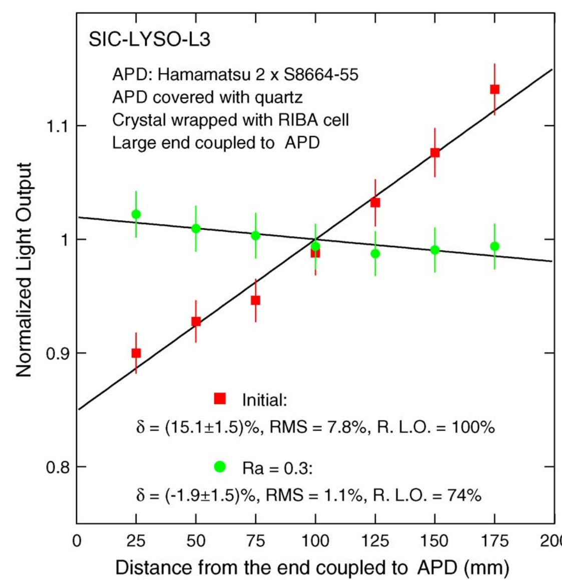

Fig. 8. Light output is shown as a function of the distance to the photo-detector for a tapered LYSO crystal before and after roughening the smallest side surface to Ra $= 0.3$.

to the photo-detector with (1) all surfaces polished; (2) one surface roughened to $\mathrm{R}_a = 0.3$ and (3) two surfaces roughened to $\mathrm{R}_a = 0.3$, where R_a is the average roughness of the surface in microns. It is clear that roughening one side surface reduces the non-uniformity from 13% to -1.3%, and roughening two side surfaces over-corrects the non-uniformity to -14%.

A recipe was chosen to roughen the smallest side surface to $\mathrm{R}_a = 0.3$. Fig. 8 shows a typical light output as a function of the distance to the photo-detector for a tapered LYSO crystal before and after roughening the smallest side surface to Ra $= 0.3$. The non-uniformity was reduced from 15% to -1.9% with corresponding light output loss of 26%. Following this test, all twenty five SuperB test beam crystals were uniformized. Fig. 9 shows a summary of the LRU measured before and after the uniformization. All twenty five crystals meet the LRU specification of $|\ \delta\ | \leq 3\%$.

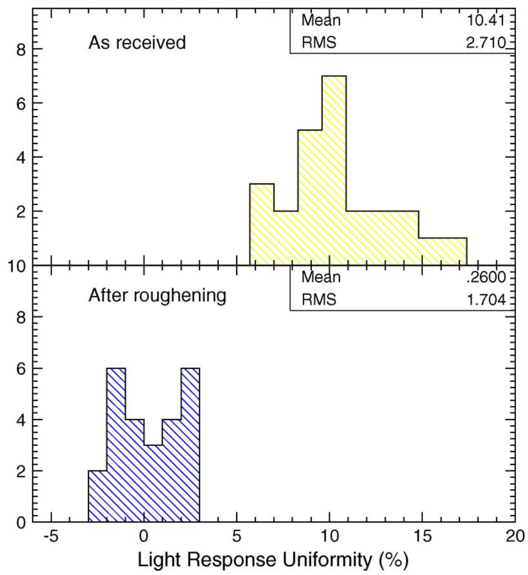

Fig. 9. LRU Summary of 25 SuperB LYSO crystals before and after one-surface roughening uniformization.

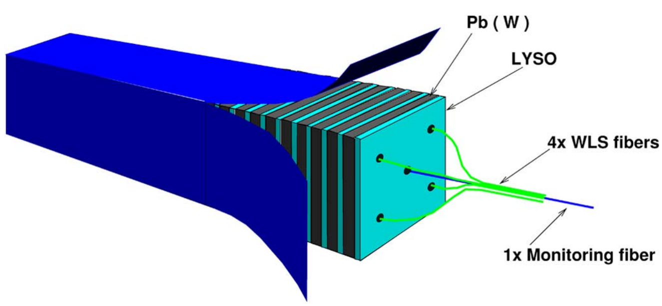

Fig. 10. Conceptual design of an LYSO-Pb Shashilik sampling calorimeter cell readout by WLS fibers.

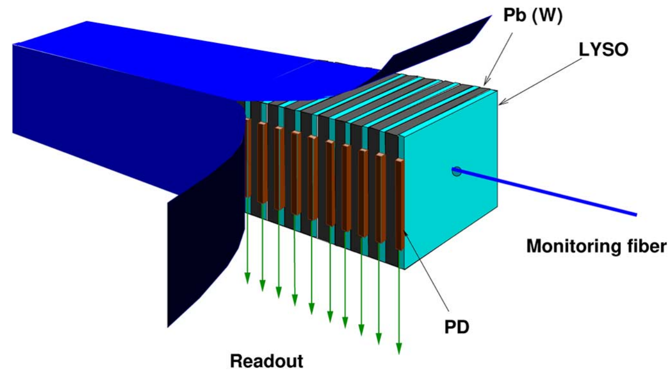

Fig. 11. Conceptual design of an LYSO-Pb sampling calorimeter cell readout by photo-detectors directly coupled to the edges of the crystal plates.

TABLE I
DESIGN OF LSO/LYSO CRYSTAL BASED SAMPLING CALORIMETER CELLS

Parameters	LYSO-Pb	LYSO-W
Number of layers	57	57
LYSO thickness (mm)	2	2
Pb or W thickness (mm)	4	2.5
Number of WLS fibers	4	4
Total depth (X_0)	25	25
Avg. Moliere radius (cm)	1.7	1.3
Avg. radiation length (cm)	0.68	0.51
Sampling fraction for MIP (%)	0.25	0.25
Total physical length (cm)	17	12.8
Transverse dimension (cm)	1.9	1.4
MIP energy in LYSO (MeV)	55	55
Total LYSO length (cm)	5.8	5.8
LYSO depth/total depth	0.2	0.2

III. LSO/LYSO CRYSTAL BASED SAMPLING ECAL

Because of its superb radiation hardness LSO/LYSO crystals are also proposed as the active material for sampling calorimeters in severe radiation environment, such as the HL-LHC [14]. Figs. 10 and 11 show two sampling calorimeter concepts with LSO/LYSO crystals as the active material. While LSO/LYSO crystals are readout by wavelength shifting (WLS) fibers in the Shashlik design, they are readout by the photo-diodes directly coupled to the edges of the LSO/LYSO crystal plates. These sampling calorimeter designs reduce the volume of LSO/LYSO crystals and thus the cost, and improve the overall radiation hardness of the calorimeter because of the much reduced light path in the sensitive materials.

An initial design of LSO/LYSO crystal based sampling calorimeter consists of 2 mm thick LYSO plates and 4 mm thick Pb or 2.5 mm thick W plates. The cells have a total depth of $25X_0$ to accommodate electrons and photons with energies up to the TeV range. The sampling fraction was chosen as 25% to provide an adequate stochastic term of the energy resolution at a level of better than 10% following GEANT simulations. Table I summarizes the main parameters of these two designs. Because of the high density of both the LSO/LYSO crystals and the absorber materials the average radiation length (0.68 cm and 0.51 cm) and Moliere radius (1.7 cm and 1.3 cm) are much smaller as compared to commonly used crystal scintillators [4]. Combined with the excellent radiation hardness of LSO/LYSO crystals, these designs provide viable solutions for stable and compact ECAL with fine granularity in a severe radiation environment, such as the HL-LHC.

A crucial issue for such sampling calorimeter is its light collection efficiency (LCE). Fig. 12 shows a setup used to measure the light output of LYSO plates. LYSO plates of $25\times$ 25 mm with thicknesses of 1.5, 3 and 5 mm were wrapped with Tyvek paper, and were readout by (1) a Hamamatsu R1306 PMT directly coupled to a large surface of the plate and (2) a Hamamatsu R2059 PMT through four 40 cm long Kuraray Y-11 WLS fibers. To allow the Y-11 WLS fiber through, four holes of 1.3 mm diameter were drilled through the plates at four positions with distances of 6.25 mm to the edges of the plate. A hole of 0.8 mm in diameter was drilled at the center of the plate to introduce monitoring laser pulses via a leaky quartz fiber [15].

Fig. 13 shows the quantum efficiencies of the Hamamatsu R1306 and R2059 PMTs used in these measurements and the emission spectra of LSO/LYSO crystals and Y-11 fibers. Also shown in the figure are the numerical values of the emission weighted quantum efficiencies (EWQE). They are 13.6% and 12.9% for LSO/LYSO and 7.3% and 7.7% for Y-11 for the R2059 and R1306 PMTs respectively.

The signals from these PMTs were digitized by a LeCroy QVT based MCA system. The light output (LO) of LSO/LYSO

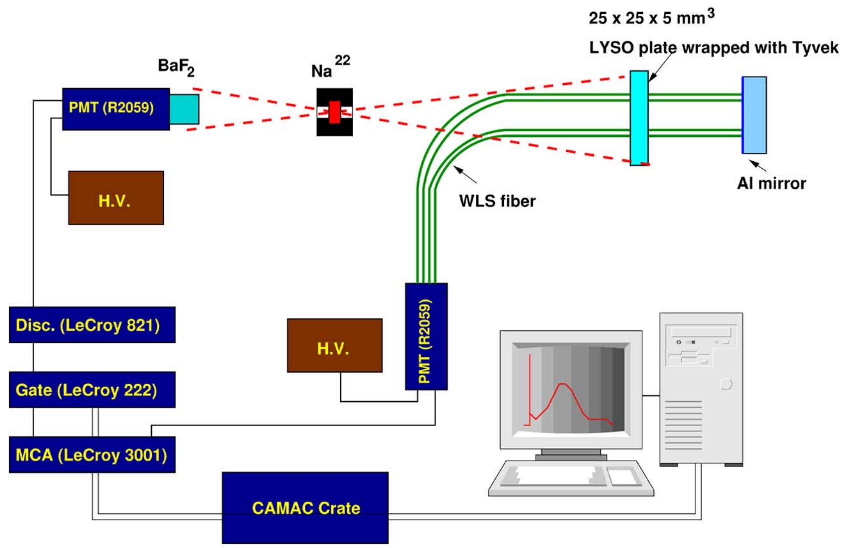

Fig. 12. Schematic showing the setup used to measure the light output of LYSO plates through four Y-11 WLS fibers.

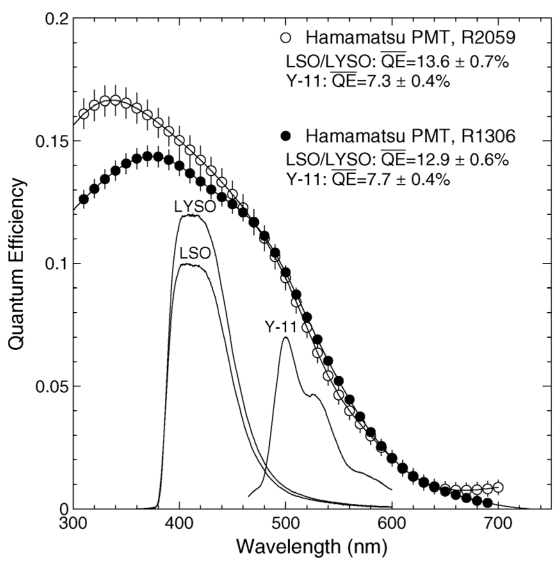

Fig. 13. Quantum efficiencies of Hamamatsu R1306 and R2059 PMTs and the emission spectra of LSO/LYSO crystals and Y-11 fibers are shown as a function of wavelength. Also shown are the corresponding EWQE.

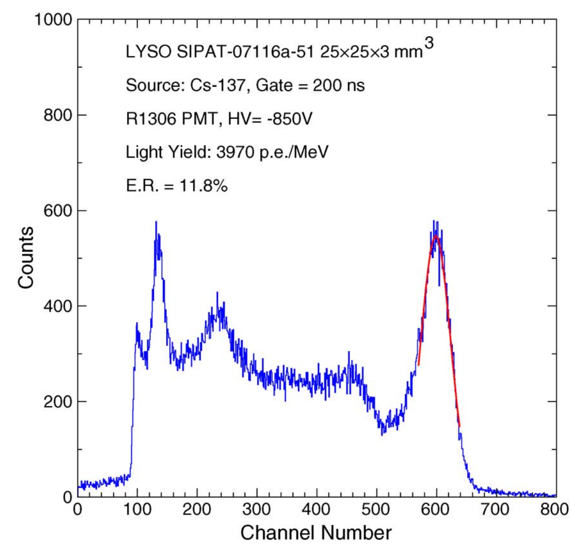

Fig. 14. A ^{137}Cs pulse height spectrum measured by a R1306 PMT for a 3.0 mm thick LYSO plate directly coupled to the PMT.

plates of different thickness were first measured by direct coupling a $25 \times 25\text{mm}^2$ surface to the R1306 PMT with Dow-Corning 200 silicone grease. Except this surface all other 5 surfaces were covered by Tyvek paper. Fig. 14 shows a ^{137}Cs pulse height spectrum measured by the R1306 PMT for a 3.0 mm thick LYSO plate directly coupled to the PMT. 3,970 p.e./MeV was measured for this plate. Taking out the 13% quantum efficiency of this PMT, the light yield was determined to be 30,780 photons/MeV.

The light output of these LYSO plates were then measured by the R2059 PMT through four Y-11 WLS fibers by using a ^{22}Na source and a coincidence trigger provided by a BaF_2 crystal as shown in Fig. 12. Fig. 15 shows a ^{22}Na pulse height spectrum measured by the R2059 PMT for a 3.0 mm thick LYSO plate. 24.3 p.e./MeV was measured for this plate. Taking out the 7.3% quantum efficiency and the air gap coupling, the photon number reaching PMT was determined to be 563 photons/MeV.

Table II summarizes light output measured for 2.5× 2.5 cm LSO/LYSO plates of three thickness, 1.5 mm, 3.0 mm and 5.0 mm, with direct coupling (LO_1 and LY_1) and through four Y-11 WLS fibers (LO_2 and LY_2), where LO refers to the light output in p.e./MeV and LY refers to the light yield in photons/MeV, i.e. with the quantum efficiency of the photo-detector taken out. The subscripts 1 and 2 refer to the readout with direct coupling and through WLS fibers respectively. It is interesting to note that the measured LCE of $\mathrm{LO}_2/\mathrm{LY}_1$ is consistent with 0.06% reported by the LHCb group for a classical Shashlik calorimeter with Pb-plastic scintillator cells [16]. The overall light collection efficiency from the LYSO scintillation photons to the photons arriving at the PMT via WLS fiber, $\mathrm{LY}_2/\mathrm{LY}_1$, is about 1.5%. The light output per minimum ionizing particle (MIP) for the designed LYSO-Pb cells is also listed in the table. Because of high light yield of LYSO, the light output per MIP in the LYSO crystal based Shashilik calorimeter cell is about six times of the plastic scintillator based LHCb Shashlik cells, which allows flexible readout designs. It is clear that

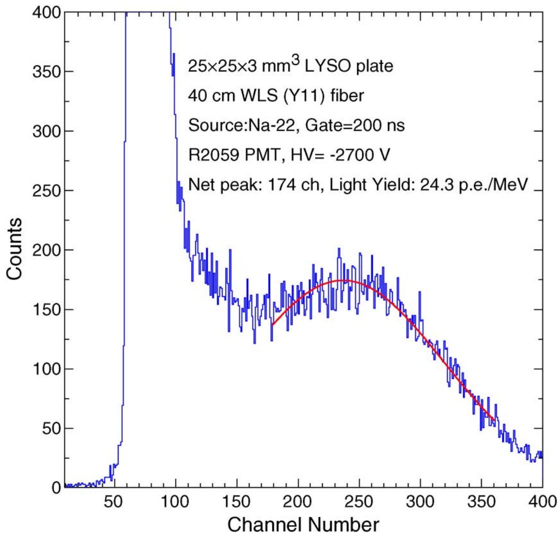

Fig. 15. A ^{22}Na pulse height spectrum measured through four Y-11 WLS fibers by a R2059 PMT for a 3.0 mm thick LYSO plate.

TABLE II
LCE OF LSO/LYSO CRYSTAL PLATES READOUT BY WLS FIBERS

LYSO Thickness	5 mm	3 mm	1.5 mm	LHCb [15]
LO_1 (p.e./MeV)	3760	3970	4370	
LY_1 (photons/MeV)	29150	30780	33880	5200
LO_2 (p.e./MeV)	20.7	24.3	17.9	3.1
LY_2 (photons/MeV)	479	563	414	
MIP (p.e./55 MeV)	1140	1340	990	169
LO_2 / LO_1 (%)	0.55	0.61	0.41	
LO_2 / LY_1 (%)	0.07	0.08	0.05	0.06
LY_2 / LY_1 (%)	1.64	1.83	1.22	

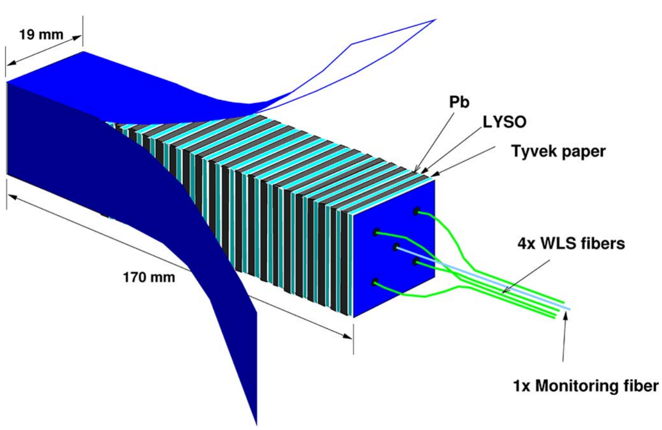

Fig. 16. Conceptual design of an LYSO crystal based Shashlik ECAL cell with lead as absorber and four Y-11 WLS fibers readout for a beam test.

LSO/LYSO crystal based sampling calorimeter provides a viable ECAL option for the proposed HL-LHC.

Fig. 16 shows a conceptual design of an LYSO crystal based Shashlik ECAL cell with lead as absorber and four Y-11 WLS fibers readout for a test beam matrix consisting of twenty five cells. Development of radiation hard WLS mechanism and photo-detectors is needed for this detector concept to be a reality for future HEP experiments at the energy frontier.

IV. SUMMARY

LSO/LYSO crystals with bright fast scintillation, small temperature dependence and excellent radiation hardness are a good candidate material for future HEP calorimeters, especially those in a severe radiation environment. The longitudinal non-uniformity issue caused by tapered crystal geometry, self-absorption and cerium segregation can be addressed by roughening one side surface. All 25 SuperB crystals are uniformized to $|\delta| \leq 3\%$ by roughening the smallest side surface to $R_a = 0.3$. LSO/LYSO crystal based Shashlik ECAL cells are designed. Three LYSO plates of 1.5, 3 and 5 mm thick were measured with direct coupling and through four Y11 WLS fibers. The overall light collection efficiency is about 1.5%, which is consistent with the existing plastic scintillator based Shashlik cells.

ACKNOWLEDGMENT

The authors would like to thank the LSO/LYSO crystal producers and colleagues from the SuperB, Mu2e and CMS experiments for many useful discussions.

REFERENCES

[1] C. Melcher, U.S. Patent 4958080 (1990) and 5025151 (1991).

[2] D. W. Cooke, K. J. McClellan, B. L. Bennett, J. M. Roper, M. T. Whittaker, and R. E. Muenchausen, "Crystal growth and optical characterization of cerium-doped $Lu_{1.8}Y_{0.2}SiO_5$," *J. Appl. Phys.*, vol. 88, pp. 7360–7362, 2000.

[3] T. Kimble, M. Chou, and B. H. T. Chai, "Scintillation properties of LYSO crystals," presented at the IEEE Nuclear Science Symp., 2002.

[4] R. H. Mao, L. Y. Zhang, and R.-Y. Zhu, "Optical and scintillation properties of inorganic scintillators in high energy physics," *IEEE Trans. Nucl. Sci.*, vol. 55, no. 4, pp. 2425–2431, Aug. 2008.

[5] R. H. Mao, L. Y. Zhang, and R.-Y. Zhu, "Gamma-ray induced radiation damage in PWO and LSO/LYSO crystals," in *Proc. IEEE Nuclear Science Symp.*, 2009, pp. 2045–2049, Paper N32-5.

[6] R. H. Mao, L. Y. Zhang, and R.-Y. Zhu, "Effect of neutron irradiations in various crystal samples of large size for future crystal calorimeter," in *Proc. IEEE Nuclear Science Symp.*, 2009, pp. 2041–2044, Paper N32-4.

[7] G. Dissertori, M. Glaser, D. Luckey, F. Nessi-Tedaldi, F. Pauss, and R. Wallny, "Results on damage induced by high-energy protons in LYSO calorimeter crystals," presented at the IEEE NSS, 2011, paper NP5.S-228, unpublished.

[8] J. Chen, R. Mao, L. Zhang, and R.-Y. Zhu, "Large size LSO and LYSO crystals for future high energy physics experiments," *IEEE Trans. Nucl. Sci.*, vol. 54, no. 3, pp. 718–724, Jun. 2007.

[9] Northern Analytical Laboratory, Inc., 13 Delta Dr. Unit #4, Londonderry, NH 03053 USA.

[10] D. A. Ma and R.-Y. Zhu, *Nucl. Instrum. Meth. A*, vol. 333, p. 422, 1993.

[11] R. Mao, L. Zhang, and R.-Y. Zhu, "Emission spectra of LSO and LYSO crystals excited by UV light, x-ray and Gamma-ray," *IEEE Trans. Nucl. Sci.*, vol. 54, no. 4, pp. 1759–1766, Jun. 2008.

[12] J. Chen, L. Zhang, and R.-Y. Zhu, "Large size LYSO crystals for future high energy physics experiments," *IEEE Trans. Nucl. Sci.*, vol. 52, no. 6, pp. 3133–3140, Dec. 2005.

[13] J. Chen, L. Zhang, and R.-Y. Zhu, "Gamma-ray induced radiation damage in large size LSO and LYSO crystals samples," *IEEE Trans. Nucl. Sci.*, vol. 54, no. 4, pp. 1319–1326, Aug. 2007.

[14] R.-Y. Zhu, "Forward calorimetry ideas," in *Proc. CMS Forward Calorimeter Task Force Meet. CERN*, Jun. 17, 2010 [Online]. Available: http://indico.cern.ch/getFile.py/access?sessionId=0&resId=4&materialId=0&confId=97272

[15] G. David, E. Kistenev, S. Stoll, S. White, and C. Woody, "The calibration and monitoring system for the PHENIX lead-scintillator electromagnetic calorimeter," *IEEE Trans. Nucl. Sci.*, vol. 45, no. 3, pp. 705–709, Jun. 1998.

[16] I. Machikhiliyan, "The LHCb electromagnetic calorimeter," in *Proc. XIII Int. Conf. Calorimeter in High Energy Physics (Calor2008)*, 2009, vol. 160, J. Phys.: Conf. Ser., p. 012047.

[17] C. Melcher and J. Schweitzer, "Cerium-doped lutetium oxyorthosilicate: A fast, efficient new scintillator," *IEEE Trans. Nucl. Sci.*, vol. 39, no. 4, pp. 502–505, Aug. 1992.